THE JOURNAL OF BIOLOGICAL CHEMISTRY VOL. 285, NO. 14, pp. 10993–11002, April 2, 2010

Kinetic Evaluation of Cell Membrane Hydrolysis during Apoptosis by Human Isoforms of Secretory Phospholipase A_2*

Received for publication, September 28, 2009, and in revised form, December 30, 2009 Published, JBC Papers in Press, February 5, 2010, DOI 10.1074/jbc.M109.070797

Erin D. Olson[‡], Jennifer Nelson[‡], Katalyn Griffith[‡], Thaothanh Nguyen[‡], Michael Streeter[‡], Heather A. Wilson-Ashworth[§], Michael H. Gelb[¶], Allan M. Judd[‡], and John D. Bell[‡1]

From the [‡]Department of Physiology and Developmental Biology, Brigham Young University, Provo, Utah 84602, the [§]Department of Biology, Utah Valley State College, Orem, Utah 84058, and the [¶]Departments of Chemistry and Biochemistry, University of Washington, Seattle, Washington 98195

Some isoforms of secretory phospholipase A_2 ($sPLA_2$) distinguish between healthy and damaged or apoptotic cells. This distinction reflects differences in membrane physical properties. Because various $sPLA_2$ isoforms respond differently to properties of artificial membranes such as surface charge, they should also behave differently as these properties evolve during a dynamic physiological process such as apoptosis. To test this idea, S49 lymphoma cell death was induced by glucocorticoid (6–48 h) or calcium ionophore. Rates of membrane hydrolysis catalyzed by various concentrations of snake venom and human groups IIa, V, and X $sPLA_2$ were compared after each treatment condition. The data were analyzed using a model that evaluates the adsorption of enzyme to the membrane surface and subsequent binding of substrate to the active site. Results were compared temporally to changes in membrane biophysics and composition. Under control conditions, membrane hydrolysis was confined to the few unhealthy cells present in each sample. Increased hydrolysis during apoptosis and necrosis appeared to reflect substrate access to adsorbed enzyme for the snake venom and group X isoforms corresponding to weakened lipid-lipid interactions in the membrane. In contrast, apoptosis promoted initial adsorption of human groups V and IIa concurrent with phosphatidylserine exposure on the membrane surface. However, this observation was inadequate to explain the behavior of the groups V and IIa enzymes toward necrotic cells where hydrolysis was reduced or absent. Thus, a combination of changes in cell membrane properties during apoptosis and necrosis capacitates the cell for hydrolysis differently by each isoform.

During programmed cell death, or apoptosis, a variety of changes occur in the plasma membrane of the cell. These include morphological alterations that emerge late in the process such as blebbing and increased permeability of the membrane. Earlier in the process, several more subtle membrane changes occur. The best studied is a loss of the normal asymmetrical transmembrane distribution of phospholipid species. Consequently, anionic lipids like phosphatidylserine, which are typically confined to the inner leaflet of the membrane, become exposed on the outer surface (1). In addition, studies with fluorescent membrane probes have revealed possible increases in fluidity and/or the spacing between lipid molecules that may precede or coincide with the loss of membrane asymmetry, depending on the cell type and mode of apoptosis (2–9). Recently, a latent increase in the order of membrane lipids has also been reported (9).

A potential consequence of these events during apoptosis is enzymatic attack of the cell membrane by secretory phospholipase A_2 ($sPLA_2$).[2] Ordinarily, healthy cells resist hydrolysis, but during apoptosis they become vulnerable to destruction by the enzyme (9–11). Studies with snake venom phospholipase A_2 have identified possible ways by which this phenomenon relates to membrane physical properties (8, 9, 12). Preliminary investigations suggest that human groups IIa (hGIIa) and V (hGV) isoforms may also distinguish healthy and apoptotic cells, although the details of how they do so are uncertain (11, 13, 14). The response of the human group X (hGX) isozyme to apoptosis has not yet been studied.

Hydrolysis of artificial membranes by $sPLA_2$ involves two precatalytic steps (Scheme 1 (15, 16)). The relationship of each step to membrane behavior varies among the different isoforms (17–20). A prominent example is the degree to which initial adsorption (step 1) depends on the presence of negative charge at the membrane surface (18, 21, 22). For instance, an anionic membrane surface appears required for pancreatic and hGIIa $sPLA_2$ (18, 23). For hGV, the presence of a tryptophan residue at the interfacial binding surface of the enzyme diminishes this requirement and allows some adsorption to a zwitterionic interface (17, 24). In the case of the hGX enzyme, there appears to be a smaller or perhaps no requirement for an anionic interface (18, 19). For snake venom $sPLA_2$ from *Agkistrodon piscivorus piscivorus*, either or both steps may be limiting depending on the physical state of the membrane (15).

This diversity of behaviors among $sPLA_2$ isoforms suggests that they would respond differently to membrane changes induced by apoptosis. For example, migration of phosphatidyl-

* This work was supported, in whole or in part, by National Institutes of Health Grant GM073997.

[1] To whom correspondence should be addressed: 302A MSRB, Brigham Young University, Provo, UT 84602. Tel.: 801-422-2353; Fax: 801-422-0263; E-mail: john_bell@byu.edu.

[2] The abbreviations used are: $sPLA_2$, secretory phospholipase A_2; hGIIa, human group IIa; hGV, human group V; hGX, human group X; AppD49, monomeric aspartate 49 $sPLA_2$ from venom of *A. p. piscivorus*; ADIFAB, acrylodan-derivatized fatty acid-binding protein; MBSS, modified balanced salt solution; GP, generalized polarization.

$$E + M_S \underset{}{\overset{K_A}{\rightleftharpoons}} E_B \underset{Ca^{2+}}{\overset{K_E \; S}{\rightleftharpoons}} E_B{}^S \xrightarrow{k_{cat}} E_B + P$$

SCHEME 1. **Reaction scheme for interaction between sPLA$_2$ and cell membranes.** *E*, free sPLA$_2$; E_B, sPLA$_2$ adsorbed to membrane surface sites (M_S); *S*, available substrate (membrane phospholipid); E_B^S, adsorbed enzyme with substrate bound to the active site; K_A, equilibrium constant for enzyme adsorption to the membrane; K_E, equilibrium constant for substrate migration into the enzyme active site; k_{cat}, catalytic rate constant for substrate hydrolysis; *P*, product (fatty acid).

serine from the inner to outer surface of the cell membrane during apoptosis is an obvious means by which sPLA$_2$ isoforms sensitive to negative charge might be capacitated to hydrolyze the membrane (25). Recent investigations have revealed additional changes such as increased interlipid spacing that may influence other isoforms (9). This study is designed to explore sPLA$_2$ species that differ in their membrane requirements and compare their response to bilayer physical properties associated with calcium ionophore and glucocorticoid-initiated apoptosis. Three human isoforms are included (hGIIa, hGV, and hGX). Snake venom (*A. p. piscivorus*) sPLA$_2$ (AppD49) is used as a standard for internal comparison to previous studies.

EXPERIMENTAL PROCEDURES

Reagents—The monomeric aspartate 9 phospholipase A2 from the venom of *A. p. piscivorus* was isolated according to the procedure of Maraganore *et al.* (26). The following recombinant human sPLA$_2$ isoforms were prepared as described previously: hGIIA (27, 28), hGV (29), and hGX (19). The hGV enzyme was generously provided by Dr. Wonhwa Cho (University of Illinois, Chicago). Dexamethasone and ionomycin were dissolved in dimethyl sulfoxide (DMSO). Acrylodan-labeled fatty acid-binding protein (ADIFAB), propidium iodide, cell culture medium, and serum were acquired from Invitrogen.

Cell Culture and Glucocorticoid Treatment—S49 mouse lymphoma cells were grown as a suspension culture at 37 °C in humidified air containing 10% CO_2 as explained (30). Samples treated with dexamethasone received the drug (100 nM final) 6–48 h before harvesting. Control samples received a corresponding volume of DMSO (0.02% v/v).

Membrane Hydrolysis—For hydrolysis assays, cells were harvested by gentle centrifugation, washed, and suspended (0.4–3.5 × 10^6 cells/ml) in a balanced salt medium (MBSS: NaCl = 134 mM, KCl = 6.2 mM, $CaCl_2$ = 1.6 mM, $MgCl_2$ = 1.2 mM, Hepes = 18.0 mM, and glucose = 13.6 mM, pH 7.4, 37 °C). Samples were transferred to quartz fluorometer sample cells and equilibrated for at least 5 min in a spectrofluorometer (Fluoromax 3, Horiba Jobin Yvon, Edison, NJ). Temperature and sample homogeneity were maintained using a water-jacketed sample chamber equipped with magnetic stirring and attached to a circulating water bath. All experiments were performed at 37 °C.

The acrylodan-derivatized fatty acid-binding protein, ADIFAB, was used to assay the release of fatty acids from cell membranes in real time. Data were acquired from cell samples 100 s (excitation = 390 nm, emission = 432 and 505 nm, bandpass = 4 nm) before adding ADIFAB (65 nM final) to assay background intensity. After the addition of ADIFAB and stabilization of the fluorescence intensity (about 300–500 s), one of the four sPLA$_2$ isoforms was added (0.07–70 nM final), and the time course was continued for an additional 800–2000 s. Fatty acid release was estimated by transforming the raw intensities to generalized polarization values (GP) and then fitting to an arbitrary function by nonlinear regression as described (31).

$$\text{ADIFAB GP} = \frac{(I_{505} - I_{432})}{(I_{505} + I_{432})} \qquad \text{(Eq. 1)}$$

I_{505} and I_{432} are the fluorescence emission intensities at 505 and 432 nm. In experiments involving calcium ionophore, ionomycin (300 nM final) or the equivalent diluent (0.25% DMSO) was included in samples with ADIFAB for at least 300 s before adding sPLA$_2$.

The intensity of propidium iodide fluorescence was used to quantify the fraction of cells susceptible to hydrolysis by sPLA$_2$ in samples treated with dexamethasone or equivalent DMSO. Cells were harvested, incubated, and mixed with sPLA$_2$ isoforms as explained above for ADIFAB experiments with differences; propidium iodide (37 μM final) was included instead of ADIFAB, fluorescence intensity was assayed at 617 nm (excitation = 536 nm), and ionomycin was added at the end of the time course to render all the cells hydrolyzable and, thus, provide a maximum signal for internal comparison (9). Data were analyzed by nonlinear regression and by quantifying the various subpopulations as described previously (9). The subpopulation of interest for this study was that in which cells were still alive (*i.e.* excluded propidium iodide) but susceptible to sPLA$_2$ (*i.e.* incorporated the dye upon the addition of sPLA$_2$). This subpopulation was quantified by calculating the difference in propidium iodide fluorescence intensity before and after the addition of sPLA$_2$ and normalizing to the maximum fluorescence change observed in samples treated with both AppD49 sPLA$_2$ and ionomycin. Data were corrected for variations in cell number using direct cell counts (by light microscopy) and light scatter intensity. Because the emission spectra of ADIFAB and propidium iodide do not overlap, the fluorescence of the two probes was assayed simultaneously for some experiments (Fig. 1) as described previously (30).

Flow Cytometry—These experiments were done in parallel with spectrofluorometric measurements of hydrolysis and propidium iodide uptake. Cells were washed and suspended in MBSS. After washing, aliquots of the control and treatment samples were transferred to flow cytometry sample tubes and incubated for 5 min with propidium iodide (10 μM final). Cell subpopulations were then identified based on the level of fluorescence intensity using a BD FACSCanto flow cytometer (BD Biosciences) with excitation at 488 nm, and emission was detected in the range of 564–606 nm.

RESULTS AND DISCUSSION

Are Subpopulations of Cells Hydrolyzed Differentially?—Fig. 1*A* displays a time course of hydrolysis of a sample of S49 cells by extracellular AppD49 sPLA$_2$. As is typical for healthy untreated samples, a small amount of fatty acid (and lysophospholipid) was produced upon the addition of sPLA$_2$ followed by a gradual return to base line as the reaction ended, and the products were salvaged by reacylation (13). This transient burst

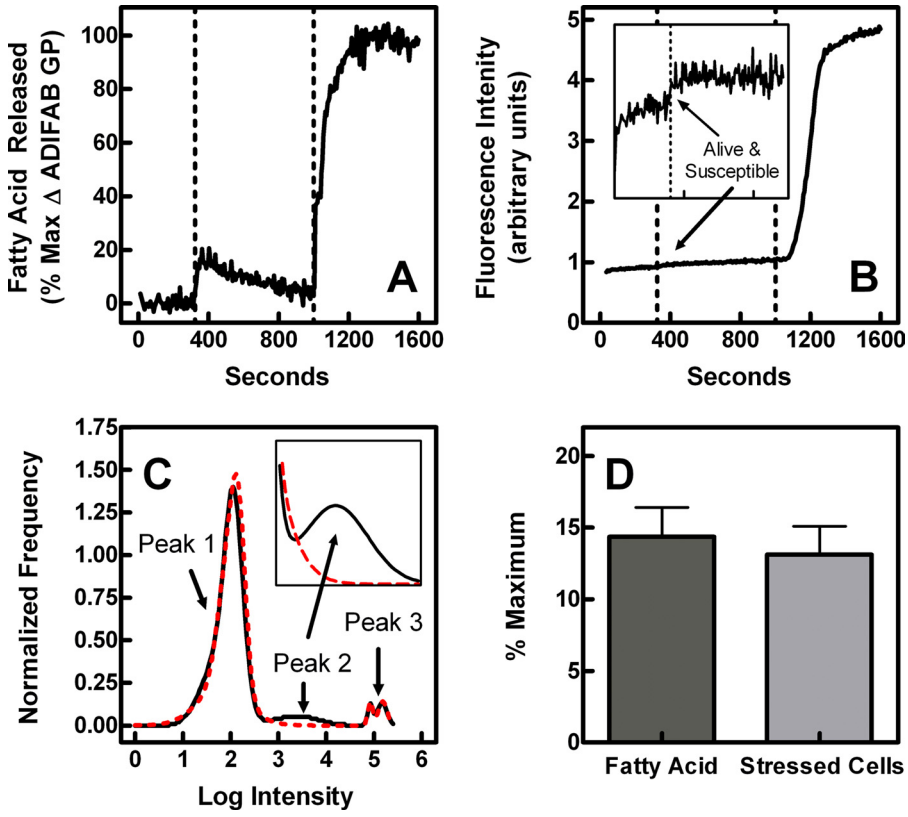

FIGURE 1. **Quantification of the cellular basis for sample hydrolysis under control conditions.** *Panel A*, hydrolysis of S49 cell membranes was assayed using ADIFAB as described under "Experimental Procedures." The amount of hydrolysis was estimated by calculating the ADIFAB GP (Equation 1) and expressing the results as a percentage of the maximum ADIFAB GP change observed in the presence of ionomycin and the AppD49 sPLA$_2$ (*plateau after the second dotted line*). *Dotted lines* represent the addition of AppD49 sPLA$_2$ (70 nM) then ionomycin (300 nM). *Panel B*, propidium iodide uptake (fluorescence intensity) was assayed simultaneously with the ADIFAB fluorescence from *Panel A*. The *inset* narrows the intensity range for the first 1000 s. *Panel C*, cell subpopulations in a companion sample were identified by flow cytometry. Peak areas were quantified by nonlinear regression using sums of multiple Gaussian distributions. *Solid black curve*, control sample; *dashed red curve*, parallel sample incubated 15 min with 70 nM AppD49 sPLA$_2$. The *inset* shows the details of Peak 2. *Panel D*, the experiments of *panels A* and *B* were repeated for a total of six samples. *Fatty Acid* represents the height of the initial hydrolysis burst (before the addition of ionomycin) in *panel A*. *Stressed Cells* represents the sum of the percentage of cells incorporating propidium iodide at the *first dotted line* in *Panel B* (*Alive & Susceptible*) plus the areas of Peaks 2 and 3 in *Panel C*. The means of the two bars were compared by paired Student's *t* test ($p = 0.74$).

of hydrolysis was accompanied by a small increase in the permeability of the cells to the fluorescent dye propidium iodide (Fig. 1*B*). Normally, healthy cells exclude the dye, but when their membranes are damaged by hydrolysis, the dye enters the cells and binds to DNA and emits with higher intensity (10). This small rise in propidium iodide fluorescence, thus, represents cells that are initially alive (impermeable) but are then killed by the action of the phospholipase (labeled *Alive & Susceptible* in the Fig. 1 *inset*). Although the increased intensity in Fig. 1*B* was very small, it was consistent with previous studies comparing healthy and apoptotic cells (10). In contrast, when ionomycin was subsequently introduced into the sample, more extensive hydrolysis was observed, as indicated by a large elevation of free fatty acid (Fig. 1*A*) and propidium iodide emission (Fig. 1*B*). The enhanced enzymatic activity and resulting membrane damage upon the addition of ionomycin represented a hydrolytic attack of 100% of the cells as the level of propidium iodide fluorescence could not be further increased by subsequent incubation of the sample with a detergent (Triton X-100, 0.25% v/v).

Interpretation of the experiments in this study requires that we determine whether the data in Fig. 1*A* represent uniform levels of hydrolysis among all the cells in the sample or extensive sensitivity of a small subpopulation of vulnerable cells. This question is of particular concern for experiments involving sPLA$_2$ because the products of hydrolysis from one cell may be able to diffuse to another cell and induce hydrolysis as has been observed with artificial membranes (32). The matter was addressed by analysis of hydrolysis time courses in the context of flow cytometry data gathered on the same samples as explained below (Figs. 1, *C* and *D*).

Previously, the transient burst of activity in control samples (Fig. 1*A*) was assumed to represent minor hydrolysis of all cells. To account for the complete cessation of hydrolysis even though substrate was restored by reacylation, a model was created in which cells become refractory after initial exposure to sPLA$_2$ (13). However, an alternative model in which a minority of the cells is susceptible to the enzyme and the remainder is resistant can also account quantitatively for the result if two assumptions are made. First, hydrolysis ceases because the membranes of vulnerable cells have been consumed. Second, uptake and reacylation of reaction products is accomplished by the remaining healthy cells in the sample.

To distinguish these possibilities, we used flow cytometry to separate healthy cell samples into subpopulations based on propidium iodide permeability (Fig. 1*C*). Data were then compared with and without sPLA$_2$ treatment to see whether all the cells were uniformly affected by the enzyme or whether certain subpopulations were preferentially altered. As shown in Fig. 1*C*, three subpopulations were identified as peaks in the flow cytometry histogram. Peak 1 represented cells that did not stain with propidium iodide. Peak 2 represented cells that displayed very low permeability to propidium iodide, an observation described for thymocytes early during apoptosis and necrosis (33, 34). Although the fluorescence intensity of these cells was 10 times that of background (Peak 1), it represented only 1% that observed for cells that were fully permeable to the dye (Peak 3). The complete permeability of the subpopulation shown in Peak 3 was confirmed by comparison to samples treated with the detergent Triton X-100 (0.1% v/v). Traditionally, cells arriving spontaneously in Peak 3 would be considered necrotic (34).

Previous studies have suggested that necrotic cells are fully susceptible to hydrolysis by sPLA$_2$ (8, 13, 30). This interpretation was confirmed indirectly using samples that contained varied proportions of necrotic cells (6–81%). Aliquots of these samples were analyzed by flow cytometry in parallel with measurements of hydrolysis using ADIFAB. A very strong correlation was observed with respect to the amount of hydrolysis and the area of Peak 3 in the flow cytometry histogram ($r^2 = 0.93$, $p < 0.0001$, $n = 9$). Moreover, the slope of the regression line was 0.91 ± 0.09, suggesting that the majority of the hydrolysis observed could be accounted for by the fully-permeable, necrotic cells of Peak 3.

We were able to assess the hydrolytic susceptibility of the cells in Peak 2 more directly because these cells were only modestly permeable to propidium iodide, and hydrolysis would, therefore, have a distinct measurable effect by making the subpopulation more permeable. Accordingly, the area defined by this part of the histogram was compared before and after treatment with sPLA$_2$. As shown by the *dashed curve* in Fig. 1*C*, Peak 2 was reduced dramatically after exposure to sPLA$_2$ ($p = 0.002$, $n = 19$), presumably because the cells had become permeabilized by the enzyme and, thus, shifted into Peak 3.

It is likely that the shallow slope of the time course in Fig. 1*B* represents the low permeability of the cells designated by Peak 2. If this is the case, the slope should be reduced after treatment with sPLA$_2$ depletes the subpopulation. In fact, the slope of the time profile was reduced by 35% ($p = 0.02$, $n = 6$) upon the addition of sPLA$_2$, again suggesting that the small burst of propidium iodide fluorescence seen in the *inset* of Fig. 1*B* represents hydrolytic attack of this tiny subpopulation.

The large population of healthy impermeable cells in Peak 1 was also analyzed as described for Peak 2. In this case, the subpopulation was mostly unaffected by sPLA$_2$; the area of Peak 1 was identical regardless of the presence of the phospholipase (Fig. 1*C*, $p = 0.21$, $n = 19$). Nevertheless, the mode of the peak was shifted slightly (7% increase in propidium iodide intensity compared with the 1000-fold increase when cells become fully permeable) but reproducibly ($p = 0.006$, $n = 19$). This result suggests that the enzyme probably does hydrolyze lipids of healthy cells but that the level is extremely small compared with the attack of the Peak 2 and Peak 3 subpopulations.

To determine whether hydrolysis of these two apparently vulnerable subpopulations could account quantitatively for the transient fatty acid release observed from ADIFAB data, we added the area of Peaks 2 and 3 and compared that sum to the size of the hydrolysis data. As shown in Fig. 1*D*, the size of these two subpopulations and the amount of hydrolysis observed in aliquots from the same samples were indistinguishable ($p = 0.74$, $n = 6$). Even though these results are based on correlation, they demonstrated that a simple model can account quantitatively for the observation of transient hydrolysis rather than having to invoke the complex ideas proposed previously (13). Therefore, we concluded that the hydrolysis of healthy cell samples by sPLA$_2$, as observed with ADIFAB fluorescence, reflects the action of the enzyme on small vulnerable subpopulations without adverse impact on the remaining cells.

Treatment of S49 cells for 18 h with dexamethasone produced a level of hydrolysis by AppD49 sPLA$_2$ intermediate between that observed in control *versus* ionomycin-treated samples (Fig. 2). As in Fig. 1*A*, subsequent addition of ionomycin induced hydrolysis of the remaining sample. Hence, as in the control samples, hydrolysis in apoptotic cells appeared confined to a sensitive subpopulation. Treatments, then, that enhance hydrolysis do so by increasing the size of the pool of susceptible cells.

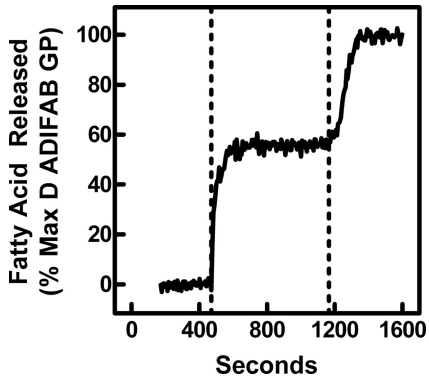

FIGURE 2. **Effect of dexamethasone treatment on the hydrolysis of S49 cell membranes by AppD49 sPLA$_2$.** The experiment of Fig. 1*A* was repeated with cells treated for 18 h with dexamethasone as explained under "Experimental Procedures."

Action of Human sPLA$_2$ Isoforms toward Apoptotic S49 Cells—Fig. 3 displays time courses of hydrolysis of S49 cell phospholipids by extracellular AppD49 (*panel A*), hGX (*panel B*), hGV (*panel C*), or hGIIa sPLA$_2$ (*panel D*) under control conditions (*black curves*). The data are expressed as a percentage of the maximum potential amount of fatty acid released as explained for Fig. 1. The hGV, hGX, and AppD49 isoforms each catalyzed a modest release of fatty acid. In contrast, no change hydrolysis was detected upon the addition of hGIIa (*panel D*).

Exposure of the cells to ionomycin produced an increase in both the rate and amount of hydrolysis by the hGV and hGX isoforms but not hGIIA (Fig. 3, *red curves*). The extent of these increases depended upon the isoform and was always less than that observed with the AppD49 enzyme (AppD49 > hGX > hGV ≫ hGIIa = 0). As shown in Fig. 4, incubation of the cells with the glucocorticoid dexamethasone for 24 h also rendered the cells susceptible to hydrolytic attack compared with cells treated with control vehicle only. In contrast to ionomycin treatment, dexamethasone was effective at causing hydrolysis of the cells by the hGIIa isoform (Fig. 4*D*).

Fig. 5 illustrates the effect of variation in enzyme concentration on the initial hydrolysis rate from experiments analogous to those of Figs. 3 and 4. The purpose of these experiments was to address the question of which steps from Scheme 1 account for the increased activity observed during apoptosis. Based on Figs. 1 and 2, the various experimental conditions used for Figs. 3–5 can be described in terms of the proportions of two subpopulations of cells: the resistant healthy subpopulation and the susceptible subpopulation. The observed initial hydrolysis rate (dP/dt), then, is the sum of the rates pertaining to each subpopulation (Res and Sus) weighted by the fraction susceptible (f_{Sus}),

$$\frac{dP}{dt_{Observed}} = (1 - f_{Sus})\frac{dP}{dt_{Res}} + f_{Sus}\frac{dP}{dt_{Sus}} \qquad \text{(Eq. 2)}$$

Explicit generic descriptions of *dP/dt* that can be applied to each subpopulation are derived as described previously (8, 12),

$$\frac{dP}{dt} = k_{cat}E_B^S \quad \text{(Eq. 3)}$$

Adsorbed enzyme with substrate occupying the active site (E_B^S) can be defined in terms of total added enzyme (E_T) and adsorption site (M_{ST}) concentrations by considering the equilibrium constants and law of conservation of mass.

$$K_A = \frac{E_B}{(E_T)(M_S)} \quad \text{(Eq. 4)}$$

$$K'_E = K_E S_T = \frac{E_B^S}{E_B} \quad \text{(Eq. 5)}$$

$$M_{ST} = M_S + E_B + E_B^S \quad \text{(Eq. 6)}$$

Substitution of Equations 4–6 into Equation 3 yields the complete generic relationship

$$\frac{dP}{dt} = \frac{k_{cat}M_{ST}K_AE_TK'_E}{1 + K_AE_T(1 + K'_E)} \quad \text{(Eq. 7)}$$

Equations 4–7 assume that the experimental conditions are designed so that most of the enzyme added remains free in solution (*i.e.* $E \approx E_T$). This assumption was verified by analysis of binding studies conducted previously with AppD49, the isoform that adsorbs most tightly to the membrane among those tested here (8). In those experiments, the amount of enzyme adsorbed to the cell surface was negligible compared with the amount that was free.

K_A and K'_E are the only constants in the equation that would be expected to vary depending on membrane structure as k_{cat} is a property of the enzyme relevant only after substrate has bound to the active site and as the total number of cells (M_{ST}) and enzyme concentration relate to the entire sample ensemble. Hence,

$$\frac{dP}{dt_{Observed}} = k_{cat}M_{ST}\left[(1 - f_{Sus})\frac{K_AE_TK'_E}{1 + K_AE_T(1 + K'_E)} + f_{Sus}\frac{K_A{}^*E_TK'_E{}^*}{1 + K_A{}^*E_T(1 + K'_E{}^*)}\right] \quad \text{(Eq. 8)}$$

where $K_A{}^*$ and $K'_E{}^*$ are the values of K_A and K'_E for the cells that have become susceptible to sPLA$_2$.

Notwithstanding the apparent complexity of Equation 8, the outcomes are straightforward depending on whether it is step one ($K_A{}^* > K_A, K'_E{}^* = K'_E$) or step two ($K_A{}^* = K_A, K'_E{}^* > K'_E$) that is rate-limiting and, therefore, responsible for low activity in healthy cells. As shown in Fig. 6, the distinction can be made by comparing different treatments in which the proportion of cells susceptible to sPLA$_2$ varies. *Panel A* displays the expected result when susceptibility induced by apoptosis relieves low adsorption affinity by increasing K_A 10-fold. The effect can be approximated by fitting the data to a traditional rectangular hyperbola function analogous to a binding isotherm or a Michaelis-Menten equation.

$$\frac{dP}{dt} = \frac{v_{max}E_T}{EC_{50} + E_T} \quad \text{(Eq. 9)}$$

As suggested by the appearance of the curves, EC_{50} varies by a factor of 5, whereas v_{max} remains nearly constant (varies by only 16%) in this case. Conversely, if step 2 is rate-limiting and apoptosis relieves that limitation by increasing K'_E (without a change in K_A), v_{max} increases proportional to the fraction of cells that have become susceptible (*panel B*), whereas EC_{50} stays essentially identical (varies by only 4%).

Accordingly, the data of Fig. 5 were fit by nonlinear regression to Equation 9. In each case, the regression was conducted as a global analysis for the three treatment groups (*blue*, DMSO control; *red*, dexamethasone; *yellow*, ionomycin). The regression was performed three different ways. First, the value of EC_{50} (*solid colored curves* in Fig. 5) was shared across the entire data set to see whether the data were accommodated when only v_{max} was allowed to vary. Second, the value of v_{max} (*dashed colored curves* in Fig. 5) was shared across the entire data set, allowing EC_{50} to float. Third, the values of both EC_{50} and v_{max} were left unconstrained to obtain an optimal fit as a standard for the other two.

The data with the AppD49 enzyme were fit better by varying v_{max} instead of EC_{50} (Fig. 5*A*). Quantitative comparison to the standard optimal fit (*black curves* in Fig. 5*A*) revealed that the correlation coefficient for the fit with v_{max} unconstrained (*solid-colored curves*) was 48-fold closer to the standard fit than was the fit with EC_{50} unconstrained (*dashed colored curves*). When v_{max} was allowed to float, its value varied significantly (95% confidence intervals: control, 0.014–0.018; dexamethasone, 0.028–0.032; ionomycin, 0.080–0.11 GP units·s^{-1}) and was greatest for ionomycin-treated samples. Thus, induction of apoptosis appeared not to affect the ability of the AppD49 enzyme to adsorb (since saturation was reached at the same concentration for each treatment). Instead, the increased v_{max} in proportion to the number of cells engaged in cell death under these conditions (control < dexamethasone < ionomycin = 100%) suggested that the second step in Scheme 1, substrate migration into the enzyme active site, was the one most facilitated by apoptosis. This conclusion substantiates interpretations reached previously for the AppD49 enzyme in model systems, human erythrocytes, and S49 cells treated with ionomycin (8, 12, 14, 15, 31).

Human group X sPLA$_2$ gave results qualitatively identical to the AppD49 enzyme (Fig. 5*B*). The correlation coefficient was 8-fold closer to the optimal standard fit when v_{max} was unconstrained instead of EC_{50}, and v_{max} values differed significantly (95% confidence intervals: control, 0.004–0.007; dexamethasone, 0.009–0.010; ionomycin, 0.012–0.019 GP units·s^{-1}). Therefore, hGX apparently also adsorbed well to the membrane surface regardless of the experimental treatment. Apoptosis presumably improved hydrolysis by enhancing substrate access to the enzyme active site, as for AppD49.

We note that a result similar to that seen for AppD49 and hGX would also be obtained if apoptosis promoted the adsorption step in the extreme; that is, negligible adsorption to healthy cells but saturation of treated cells. However, several lines of evidence argue against this alternative. Binding experiments

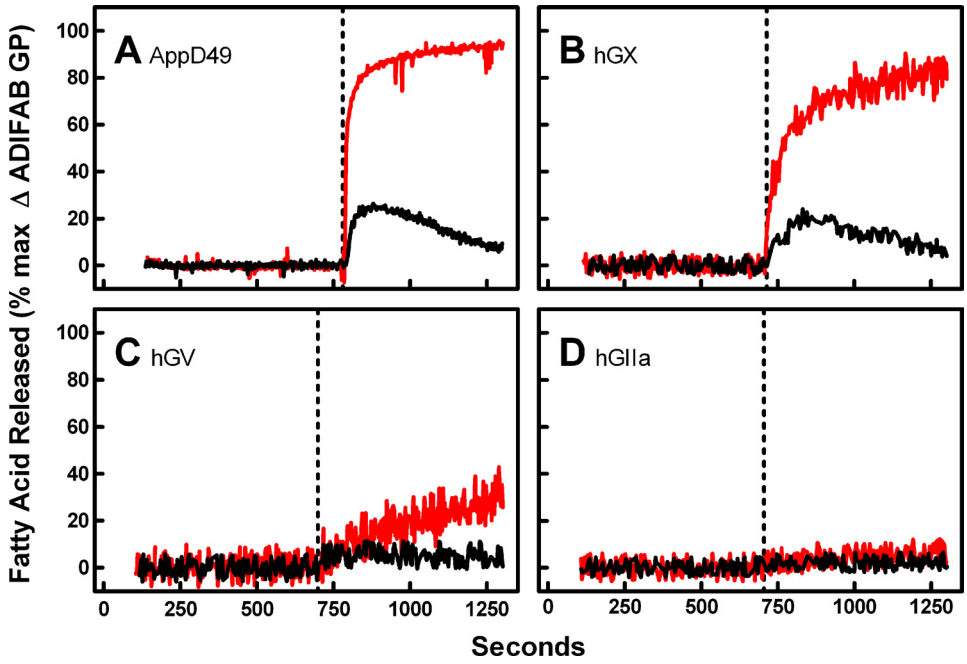

FIGURE 3. **Hydrolysis of S49 cell membranes by different sPLA$_2$ isoforms in the presence and absence of ionomycin.** S49 cells were incubated with ADIFAB and treated for at least 300 s with DMSO (*black curves*, 0.25% v/v, control solvent for drugs) or ionomycin (*red curves*, 300 nM) before the addition of sPLA$_2$ (*dotted lines*) as in Fig. 1*A*. *A*, 35 nM AppD49; *B*, 35 nM hGX; *C*, 35 nM hGV; *D*, 70 nM hGIIa.

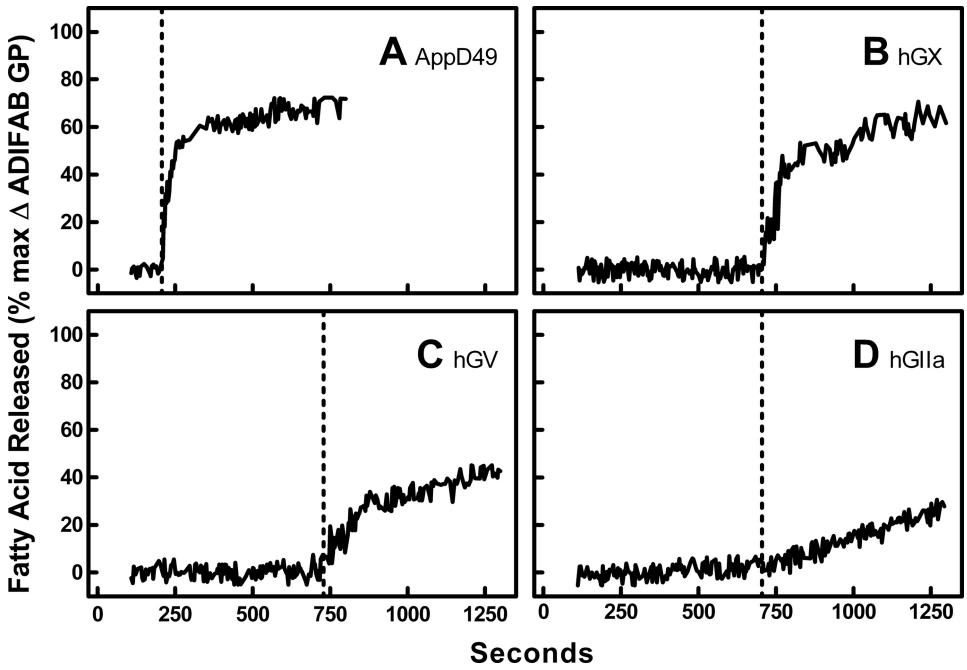

FIGURE 4. **Effects of dexamethasone treatment on the time course of membrane hydrolysis by sPLA$_2$.** The experiments of Fig. 3 were repeated with cells that had previously been treated for 24 h with dexamethasone (100 nM) instead of DMSO or ionomycin. The *dotted lines* indicate the addition of sPLA$_2$. *A*, 35 nM AppD49; *B*, 35 nM hGX; *C*, 35 nM hGV; *D*, 70 nM hGIIa.

have demonstrated that the AppD49 enzyme adsorbs equally well to treated and untreated cell membranes (8, 12). Likewise, previous studies have observed high affinity adsorption of hGX sPLA$_2$ to zwitterionic artificial membranes and to non-apoptotic cells (18, 21, 35). Thus, the interpretation that step two is limiting for these isozymes seems to be the most plausible explanation for the data.

In contrast to AppD49 and hGX, the data for the hGV isoform were better fit by Equation 9 when EC_{50} was varied rather than v_{max} (*dashed curves* Fig. 5*C*). In this case, the correlation coefficient was 18-fold closer to the optimal standard fit when EC_{50} was unconstrained. The value of EC_{50} varied from 154 nM (95% confidence interval = 150–158 nM) in control samples to 87 nM (76–98 nM) in ionomycin-treated samples and reached 24 nM (10–38 nM) for cells treated with dexamethasone. Thus, the ability of the hGV isoform to adsorb to the membrane was increased during apoptosis.

The data for hydrolysis by hGIIa did not match the functional form of Equation 9, as illustrated by the upward concavity of the curves (Fig. 5*D*). The lack of a plateau in the data indicated that adsorption of the enzyme was weak and that saturation of the cell surface was not achieved at any of the concentrations tested. Nevertheless, the enzyme responded with the highest potency to cells treated with dexamethasone, analogous to the behavior of hGV. This result also suggests that there was virtually no adsorption of hGIIa to untreated cells as has been suggested previously (35) and that ionomycin treatment did little or nothing to alter that condition.

Relationship to Physical Changes in the Membrane—The underlying assumption in these investigations is that changes occur in the composition and/or physical structure of the cell membrane during apoptosis that facilitate whatever step(s) in Scheme 1 is limiting in healthy untreated cells. Because different steps appear critical for different isoforms, it is also likely that the various enzymes are also sensitive to different physical membrane properties. Therefore, the timing of onset of hydrolysis during apoptosis should vary among the isoforms and correspond temporally with the relevant physical changes. Accordingly, we compared the rate of hydrolysis (Fig. 7) and fraction of cells still alive but susceptible to sPLA$_2$ (Fig. 8) as a function of treatment time with dexamethasone for each of the isoforms. These time profiles were then compared with the timing of previously mea-

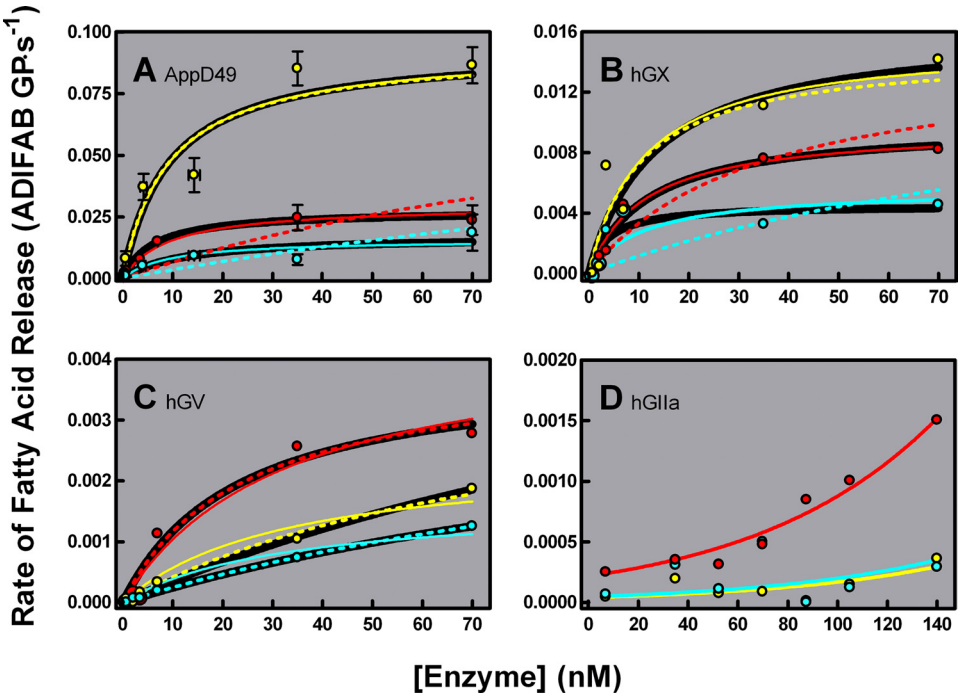

FIGURE 5. **Dependence of the initial rate of hydrolysis on sPLA$_2$ concentration.** The experiments of Figs. 3 and 4 were repeated at the indicated concentrations of sPLA$_2$ for cells treated with DMSO (*blue symbols* and *curves*), ionomycin (*yellow*), or dexamethasone (*red*). The initial rates were calculated from the amount of product generated during the first 5 s (AppD49 (*A*)), 20 s (hGX (*B*)), or 50 s (hGV (*C*) and hGIIa (*D*)) after sPLA$_2$ addition ($n = 1$–14). *Error bars* represent the S.E. (when $n > 2$) or range (when $n = 2$). Data in *Panels A–C* were fit by nonlinear regression to Equation 9 with the constraint that either the parameter value for EC_{50} (*solid colored curves*) or v_{max} (*dashed colored curves*) was shared and, therefore, constant among the three data sets. The *black curves* in *panels A–C* depict fits in which neither EC_{50} nor v_{max} was constrained.

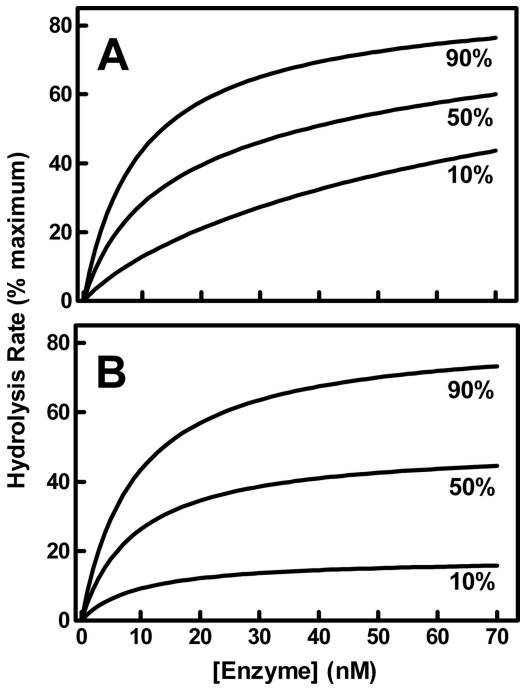

FIGURE 6. **Theoretical description of kinetic behavior of sPLA$_2$ depending on whether apoptosis promotes step 1 (*panel A*) or step 2 (*panel B*).** Data were calculated using Equation 8 for values of f_{sus} corresponding to susceptible subpopulations representing 90, 50, or 10% of the cell sample. In *panel A*, $K_A = 0.01$ nM^{-1}, $K'_E = 0.1$; in *panel B*, $K_A = 0.1$ nM^{-1}, $K'_E = 0.01$. The other parameter values were $k_{cat} = 1$ unit·s^{-1}, $M_{ST} = 1000$ arbitrary units, $K_A{}^* = 0.1$ nM^{-1}, and $K'_E{}^* = 0.1$.

sured membrane changes during dexamethasone-stimulated apoptosis (Fig. 9).

Prolonged treatment with DMSO (up to 48 h) had no effect on the kinetics of membrane hydrolysis by AppD49 sPLA$_2$ as long as cell viability did not diminish. Dexamethasone treatment produced a biphasic enhancement of hydrolysis with maximum activity observed at 18–24 h (Fig. 7*A*). The data at this mid time range were distinguishable from control (*horizontal dotted line*) by *t* test ($p = 0.003$); the pooled values for early (6–12 h) and late (30–48 h) time points were not significant.

The human isoforms displayed results comparable with the AppD49. In each case, the hydrolysis rate reached a maximum around 18–24 h of dexamethasone treatment, although the onset of elevated activity appeared sooner for the AppD49 and hGX enzymes than for hGIIa and hGV isoforms. On the other hand, hGIIa and hGV behaved like the snake venom at long time points at which the amount of hydrolysis observed receded to the same as control levels (Figs. 7, *C* and *D*), whereas hGX activity remained elevated (albeit at a diminished level compared with the peak; Fig. 7*B*).

As revealed by Fig. 1*B*, a small portion of the cells that are hydrolyzed by sPLA$_2$ during apoptosis is still alive but have become vulnerable to the enzyme. This small fraction represents an important observation because it demonstrates that the onset of membrane susceptibility to sPLA$_2$ occurs during the biochemical process of apoptosis rather than being merely an end point state of dead cells (9, 10). Fig. 8 shows that this phenomenon was not confined solely to the AppD49 enzyme, but instead, it was similar both in timing (peak at ~6–12 h) and magnitude (~2–4% at peak, 7–14% integrated total) among the human isozymes tested. The earliness of the peak is consistent with the assumption that these cells are not yet dead even though they have initiated the process of apoptosis.

Three molecular-level membrane changes have been identified previously during dexamethasone-induced apoptosis in S49 cells (9). They are 1) a reduction in the strength of interactions among neighboring lipids, assessed by merocyanine and laurdan fluorescence, 2) a latent increase in the order of membrane lipids, assayed by laurdan and diphenylhexatriene fluorescence, and 3) exposure of the anionic phospholipid phosphatidylserine on the outer leaflet of the cell membrane identified by the binding of annexin V. The time courses of these changes are represented in Fig. 9 where they are compared with the hydrolysis profiles from Fig. 7 to identify possible mechanisms to account for the hydrolytic behavior.

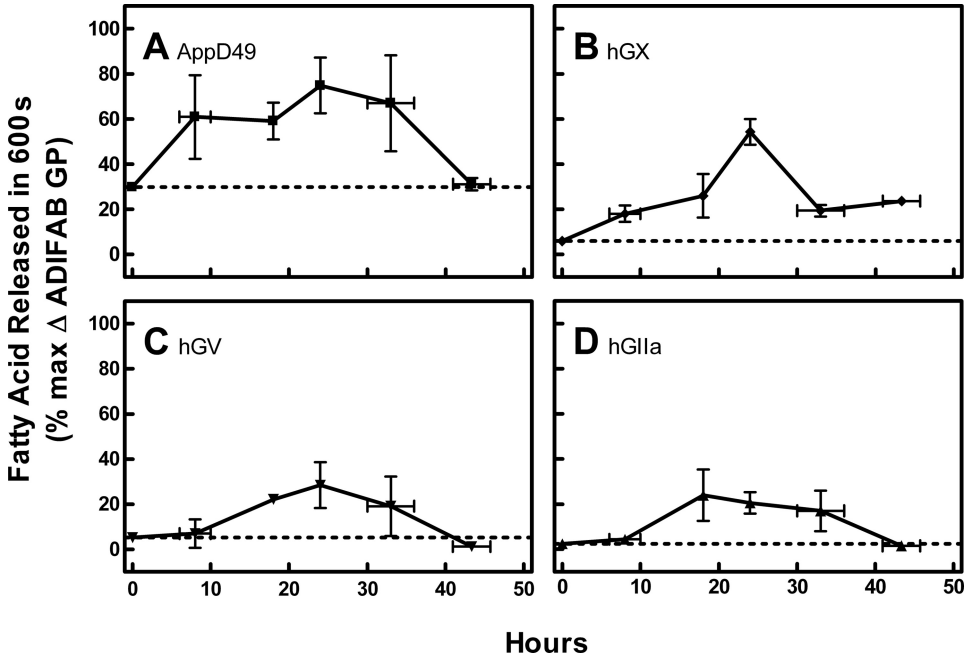

FIGURE 7. **Effect of dexamethasone treatment time on hydrolysis of S49 cell membranes by sPLA$_2$.** The total amount of hydrolysis observed after 600 s was assessed for each isoform (35 nM) from experiments such as those in Fig. 4 with cells treated for 6–48 h with 100 nM dexamethasone ($n = 2$–4). *Dotted lines* represent the average control (DMSO) value for each isoform. *Error bars* represent the S.E. (when $n > 2$) or range (when $n = 2$). Early (<15 h), mid (15–30 h), and late (>30 h) segments of the time course were evaluated by one-sample *t* tests with H_0 = control value. In each panel the mid group was statistically significant ($p \leq 0.01$). The late group was also significant in *panel B* ($p = 0.0005$). *A*, AppD49; *B*, hGX; *C*, hGV; *D*, hGIIa.

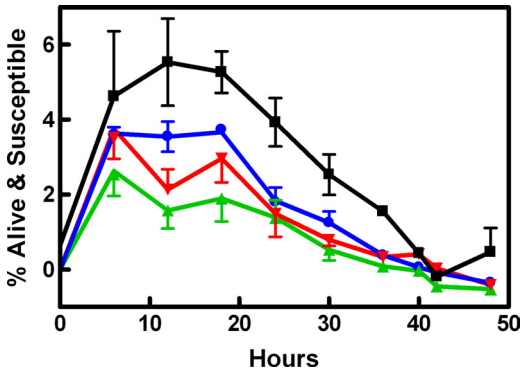

FIGURE 8. **Percent of cells identified as alive and susceptible to sPLA$_2$ using propidium iodide as a probe of membrane integrity.** S49 cells were treated for the indicated times with dexamethasone (100 nM), and the percentage of cells alive but susceptible to AppD49 (*black*), hGIIa (*green*), hGV (*red*), or hGX (*blue*) was calculated as explained under "Experimental Procedures" ($n = 1$–15). See the *inset* to Fig. 1*B* for visual definition of *Alive & Susceptible* population. *Error bars* represent the S.E. (when $n > 2$) or range (when $n = 2$).

The temporal correspondence between these events and hydrolysis was striking. Fig. 9*A* superimposes the hydrolysis time profile by hGX. The initial rise in activity corresponded exactly with the initial lowering of lipid-neighbor interactions detected by merocyanine 540 (*blue curve*). A secondary increase in activity observed with both AppD49 and hGX between 18 and 24 h coincided with the rising exposure of phosphatidylserine (*green curve*). The downward trend at longer time points appeared to be explained by the latent increase in membrane order (*red curve*). Collectively, these observations were consistent with previous *in vivo* and *in vitro* studies with the snake venom enzyme (8, 12, 14, 15, 31) and suggest that the behavior of hGX is the same as that proposed for the venom as follows. 1) Catalytic activity toward cell membranes is limited by step 2 in Scheme 1. 2) This limitation is relieved by diminished interactions among neighboring phospholipids, which facilitate upward migration of phospholipids into the active site of adsorbed enzyme. 3) Anionic phospholipids are not required for enhanced hydrolytic activity during apoptosis, but they help. 4) A highly ordered membrane impairs activity.

In contrast, reduced interlipid interactions (*blue curve* in Fig. 9*B*) were either irrelevant or insufficient to explain enhanced activity of the hGIIa and hGV isozymes. Exposure of phosphatidylserine (*green curve*), however, corresponded exactly with the enhanced activity until membrane order began to change (*red curve*). This result matched well with the observation that the activity of these isoforms seemed limited by their affinity for the membrane surface (step 1 in Scheme 1) and because *in vitro* studies indicate that these enzymes have a strong (hGV) or absolute (hGIIa) requirement for negative charge on the membrane surface (17, 18, 21, 25, 35–37). As with the other isoforms, the highly ordered cell membranes present during the late phase of apoptosis appeared to inhibit hydrolytic activity and override the beneficial effect of phosphatidylserine exposure.

In contradistinction to dexamethasone, ionomycin treatment immediately (within 10 min) induces 100% of the cells to experience both the reduction in lipid-neighbor interactions and maximal exposure of phosphatidylserine (10). This result seems adequate to explain the high level of hydrolysis observed with the AppD49 and hGX enzymes toward ionomycin-treated cells (*i.e.* as in Figs. 1, 3, and 5). However, the observation that ionomycin treatment had essentially no effect on hydrolysis by hGIIa and a weak effect on hGV was a complete surprise. As argued in the previous paragraph, the observations with dexamethasone treatment strongly supported the hypothesis that hydrolysis by these enzymes is capacitated by exposure of phosphatidylserine on the cell surface. Thus, one would have expected ionomycin treatment to stimulate both isozymes strongly as it produces maximum exposure of phosphatidylserine (*i.e.* twice that observed at 24 h with dexamethasone). Clearly, some unidentified membrane event associated with ionomycin treatment impairs the binding and activity of hGIIa and hGV, or some additional event during glucocorticoid treatment is required beyond phosphatidylserine exposure.

The nature of this implied difference between the membrane behavior provoked by glucocorticoid and calcium ionophore

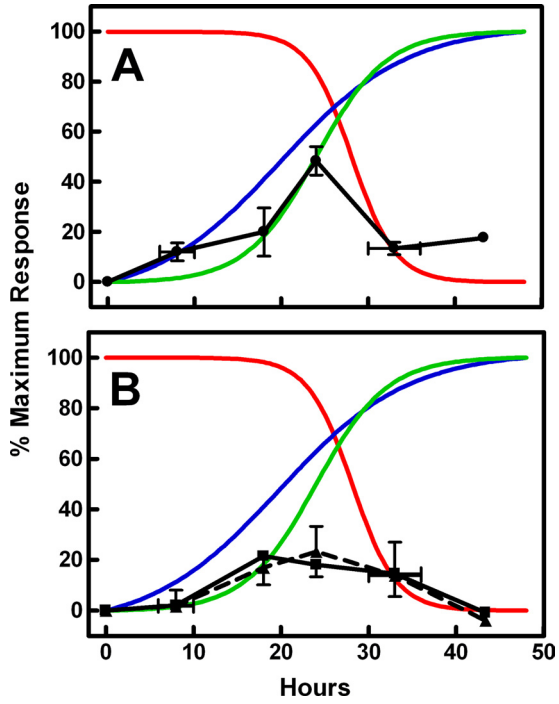

FIGURE 9. **Comparison of susceptibility levels to physical changes in the cell membrane during dexamethasone-stimulated apoptosis.** *Panel A*, the data of Fig. 7*B* were superimposed with measurements of interlipid spacing (*blue curve*), phosphatidylserine exposure (*green curve*), and membrane disorder (*red curve*). The three curves are nonlinear regressions of multiple experimental data points (96 for *blue*, 31 for *green*, and 26 for *red*) reported in Bailey *et al.* (9). Interlipid spacing was assessed by merocyanine 540 fluorescence; a similar response was obtained by two-photon microscopy using laurdan (9). Phosphatidylserine exposure on the outer leaflet of the cell membrane was assessed by flow cytometry using annexin V as a probe. Membrane disorder was observed jointly by diphenylhexatriene anisotropy and laurdan fluorescence. *Panel B*, the data of Figs. 7, *C* and *D*, were superimposed on the same curves from *panel A*.

treatments is unknown, although a few clues may be gleaned from prior investigations. For example, oxidation of membrane lipids during apoptosis is one candidate for this mystery factor for which there is some experimental precedence (38–44). Moreover, some studies of the features of cell death induced by ionomycin treatment argue that it stimulates a process more akin to necrosis than to typical apoptosis (45, 46). For example, even though ionomycin eventually stimulates uptake of propidium iodide into S49 cells, it does not produce DNA fragmentation (10). It is also likely that some of the susceptible subpopulation in control samples represents necrotic cells because of the absence of apoptotic stimuli. If these statements concerning necrosis are true, then a primary difference among the human sPLA$_2$ isoforms may be their relative ability to recognize and digest cells engaged in necrotic demise; *i.e.* the hGX isozyme strongly hydrolyzes necrotic cells, hGV does so to a lesser extent, and hGIIa seems nearly incapable of recognizing necrotic cells.

Concluding Remarks—This study provides evidence that biophysical and kinetic investigations with sPLA$_2$ using artificial and cell membranes under basic experimental conditions are pertinent to the action of human forms of the enzyme toward living nucleated cells in a physiological and/or pathological setting. Previous studies with simplified systems have argued that basic membrane properties such as lipid packing density and surface charge are fundamental determinants of the ability of this enzyme to function at the bilayer surface (8, 12, 14, 15, 17, 18, 21, 23, 25, 31, 35–37, 47). Such studies are commonly criticized with respect to their relevance to complex biological systems. This study addresses that criticism by applying the biophysical information gleaned from model systems and with model enzymes (such as snake venom sPLA$_2$) to the process of programmed cell death and human isozymes. Although, these results relate specifically to S49 lymphoma cells, observations of sPLA$_2$-catalyzed hydrolysis of various other cell lines during apoptosis or necrosis suggest that they apply broadly (10, 11, 13, 35, 48, 49).

In summary, there are five novel conclusions resulting from the data of this project. First, the properties of healthy cell membranes naturally resist hydrolysis by all three human sPLA$_2$ isoforms tested. However, all three isoforms actively hydrolyze the membranes of cells rendered apoptotic by glucocorticoid. Second, the hGX isoform appears to benefit from a reduction in the strength of interactions among neighboring lipids resulting in easier migration of phospholipids into the enzyme active site. Third, although this reduction in packing density may be sufficient for hGX sPLA$_2$, the hGV and hGIIa isozymes appear to require an additional alteration that improves the ability of these enzymes to adsorb to the membrane surface. This additional alteration is probably the exposure of phosphatidylserine on the membrane surface. Fourth, in addition to glucocorticoid-stimulated apoptosis, cell damage from calcium influx also renders the membranes susceptible to hGX and (to a lesser extent) hGV but not hGIIa. The relevant distinguishing element between death caused by calcium influx and glucocorticoid is not yet known. Fifth, for hGV and hGIIa isoforms, the ability to hydrolyze cells during apoptosis is transient. The highly ordered cell corpses appear to be substrates (albeit weaker) only for hGX.

These conclusions imply possible physiological roles for the three human isoforms. The fact that all three ignore or display reduced activity toward healthy cells is beneficial because they are capable of killing cells by inflicting membrane damage and because the hydrolysis products are proinflammatory. All three are potentially bactericidal and, hence, may play a role in the innate immune system (50–56). In addition, the hGX isoform appears capable of performing a general role for clearing damaged cells and cellular debris after traumatic injury. The hGV and especially the hGIIa isoforms, in contrast, may only generate significant hydrolysis of apoptotic cells.

Acknowledgments—We thank Wonhwa Cho of the University of Illinois, Chicago, for generously providing samples of hGV sPLA$_2$ and Ashley Warcup of Brigham Young University for technical assistance.

REFERENCES

1. Fadeel, B. (2004) *Antioxid. Redox Signal.* **6,** 269–275
2. Mower, D. A., Jr., Peckham, D. W., Illera, V. A., Fishbaugh, J. K., Stunz, L. L., and Ashman, R. F. (1994) *J. Immunol.* **152,** 4832–4842
3. Jourd'heuil, D., Aspinall, A., Reynolds, J. D., and Meddings, J. B. (1996) *Can. J. Physiol. Pharmacol.* **74,** 706–711
4. Fujimoto, K., Iwasaki, C., Kawaguchi, H., Yasugi, E., and Oshima, M. (1999) *FEBS Lett.* **446,** 113–116

5. Raghavendra, P. B., Sreenivasan, Y., and Manna, S. K. (2007) *Mol. Immunol.* **44,** 2292–2302
6. Baritaki, S., Apostolakis, S., Kanellou, P., Dimanche-Boitrel, M. T., Spandidos, D. A., and Bonavida, B. (2007) *Adv. Cancer Res.* **98,** 149–190
7. Moulin, M., Carpentier, S., Levade, T., and Arrigo, A. P. (2007) *Apoptosis.* **12,** 1703–1720
8. Bailey, R. W., Olson, E. D., Vu, M. P., Brueseke, T. J., Robertson, L., Christensen, R. E., Parker, K. H., Judd, A. M., and Bell, J. D. (2007) *Biophys. J.* **93,** 2350–2362
9. Bailey, R. W., Nguyen, T., Robertson, L., Gibbons, E., Nelson, J., Christensen, R. E., Bell, J. P., Judd, A. M., and Bell, J. D. (2009) *Biophys. J.* **96,** 2709–2718
10. Nielson, K. H., Olsen, C. A., Allred, D. V., O'Neill, K. L., Burton, G. F., and Bell, J. D. (2000) *Biochim. Biophys. Acta* **1484,** 163–174
11. Atsumi, G., Murakami, M., Tajima, M., Shimbara, S., Hara, N., and Kudo, I. (1997) *Biochim. Biophys. Acta* **1349,** 43–54
12. Jensen, L. B., Burgess, N. K., Gonda, D. D., Spencer, E., Wilson-Ashworth, H. A., Driscoll, E., Vu, M. P., Fairbourn, J. L., Judd, A. M., and Bell, J. D. (2005) *Biophys. J.* **88,** 2692–2705
13. Wilson, H. A., Waldrip, J. B., Nielson, K. H., Judd, A. M., Han, S. K., Cho, W., Sims, P. J., and Bell, J. D. (1999) *J. Biol. Chem.* **274,** 11494–11504
14. Smith, S. K., Farnbach, A. R., Harris, F. M., Hawes, A. C., Jackson, L. R., Judd, A. M., Vest, R. S., Sanchez, S., and Bell, J. D. (2001) *J. Biol. Chem.* **276,** 22732–22741
15. Henshaw, J. B., Olsen, C. A., Farnbach, A. R., Nielson, K. H., and Bell, J. D. (1998) *Biochemistry* **37,** 10709–10721
16. Gelb, M. H., Jain, M. K., Hanel, A. M., and Berg, O. G. (1995) *Annu. Rev. Biochem.* **64,** 653–688
17. Han, S. K., Kim, K. P., Koduri, R., Bittova, L., Munoz, N. M., Leff, A. R., Wilton, D. C., Gelb, M. H., and Cho, W. (1999) *J. Biol. Chem.* **274,** 11881–11888
18. Singer, A. G., Ghomashchi, F., Le Calvez, C., Bollinger, J., Bezzine, S., Rouault, M., Sadilek, M., Nguyen, E., Lazdunski, M., Lambeau, G., and Gelb, M. H. (2002) *J. Biol. Chem.* **277,** 48535–48549
19. Pan, Y. H., Yu, B. Z., Singer, A. G., Ghomashchi, F., Lambeau, G., Gelb, M. H., Jain, M. K., and Bahnson, B. J. (2002) *J. Biol. Chem.* **277,** 29086–29093
20. Beers, S. A., Buckland, A. G., Giles, N., Gelb, M. H., and Wilton, D. C. (2003) *Biochemistry* **42,** 7326–7338
21. Bezzine, S., Bollinger, J. G., Singer, A. G., Veatch, S. L., Keller, S. L., and Gelb, M. H. (2002) *J. Biol. Chem.* **277,** 48523–48534
22. Bell, J. D., and Biltonen, R. L. (1989) *J. Biol. Chem.* **264,** 225–230
23. Jain, M. K., Yu, B. Z., and Kozubek, A. (1989) *Biochim. Biophys. Acta* **980,** 23–32
24. Han, S. K., Yoon, E. T., and Cho, W. (1998) *Biochem. J.* **331,** 353–357
25. Murakami, M., Kambe, T., Shimbara, S., Higashino, K., Hanasaki, K., Arita, H., Horiguchi, M., Arita, M., Arai, H., Inoue, K., and Kudo, I. (1999) *J. Biol. Chem.* **274,** 31435–31444
26. Maraganore, J. M., Merutka, G., Cho, W., Welches, W., Kézdy, F. J., and Heinrikson, R. L. (1984) *J. Biol. Chem.* **259,** 13839–13843
27. Baker, S. F., Othman, R., and Wilton, D. C. (1998) *Biochemistry* **37,** 13203–13211
28. Markova, M., Koratkar, R. A., Silverman, K. A., Sollars, V. E., MacPhee-Pellini, M., Walters, R., Palazzo, J. P., Buchberg, A. M., Siracusa, L. D., and Farber, S. A. (2005) *Oncogene* **24,** 6450–6458
29. Cho, W., Han, S. K., Lee, B. I., Snitko, Y., and Dua, R. (1999) *Methods Mol. Biol.* **109,** 31–38
30. Wilson, H. A., Huang, W., Waldrip, J. B., Judd, A. M., Vernon, L. P., and Bell, J. D. (1997) *Biochim. Biophys. Acta* **1349,** 142–156
31. Harris, F. M., Smith, S. K., and Bell, J. D. (2001) *J. Biol. Chem.* **276,** 22722–22731
32. Bell, J. D., Brown, S. D., and Baker, B. L. (1992) *Biochim. Biophys. Acta* **1127,** 208–220
33. Lyons, A. B., Samuel, K., Sanderson, A., and Maddy, A. H. (1992) *Cytometry* **13,** 809–821
34. Vitale, M., Zamai, L., Mazzotti, G., Cataldi, A., and Falcieri, E. (1993) *Histochemistry* **100,** 223–229
35. Bezzine, S., Koduri, R. S., Valentin, E., Murakami, M., Kudo, I., Ghomashchi, F., Sadilek, M., Lambeau, G., and Gelb, M. H. (2000) *J. Biol. Chem.* **275,** 3179–3191
36. Kinkaid, A. R., and Wilton, D. C. (1995) *Biochem. Soc. Trans.* **23,** 556S
37. Koduri, R. S., Baker, S. F., Snitko, Y., Han, S. K., Cho, W., Wilton, D. C., and Gelb, M. H. (1998) *J. Biol. Chem.* **273,** 32142–32153
38. Chang, M. K., Binder, C. J., Miller, Y. I., Subbanagounder, G., Silverman, G. J., Berliner, J. A., and Witztum, J. L. (2004) *J. Exp. Med.* **200,** 1359–1370
39. Kagan, V. E., Gleiss, B., Tyurina, Y. Y., Tyurin, V. A., Elenström-Magnusson, C., Liu, S. X., Serinkan, F. B., Arroyo, A., Chandra, J., Orrenius, S., and Fadeel, B. (2002) *J. Immunol.* **169,** 487–499
40. Salgo, M. G., Corongiu, F. P., and Sevanian, A. (1993) *Arch. Biochem. Biophys.* **304,** 123–132
41. Sevanian, A., Wratten, M. L., McLeod, L. L., and Kim, E. (1988) *Biochim. Biophys. Acta* **961,** 316–327
42. Tyurin, V. A., Tyurina, Y. Y., Jung, M. Y., Tungekar, M. A., Wasserloos, K. J., Bayir, H., Greenberger, J. S., Kochanek, P. M., Shvedova, A. A., Pitt, B., and Kagan, V. E. (2009) *J. Chromatogr. B Analyt. Technol. Biomed. Life Sci.* **877,** 2863–2872
43. Tyurin, V. A., Tyurina, Y. Y., Feng, W., Mnuskin, A., Jiang, J., Tang, M., Zhang, X., Zhao, Q., Kochanek, P. M., Clark, R. S., Bayir, H., and Kagan, V. E. (2008) *J. Neurochem.* **107,** 1614–1633
44. Tyurin, V. A., Tyurina, Y. Y., Kochanek, P. M., Hamilton, R., DeKosky, S. T., Greenberger, J. S., Bayir, H., and Kagan, V. E. (2008) *Methods Enzymol.* **442,** 375–393
45. Gwag, B. J., Canzoniero, L. M., Sensi, S. L., Demaro, J. A., Koh, J. Y., Goldberg, M. P., Jacquin, M., and Choi, D. W. (1999) *Neuroscience* **90,** 1339–1348
46. Kottilil, S., Bowmer, M. I., Trahey, J., Howley, C., Gamberg, J., and Grant, M. D. (2001) *Cell. Immunol.* **214,** 1–11
47. Demel, R. A., Geurts van Kessel, W. S., Zwaal, R. F., Roelofsen, B., and van Deenen, L. L. (1975) *Biochim. Biophys. Acta* **406,** 97–107
48. Fourcade, O., Simon, M. F., Viodé, C., Rugani, N., Leballe, F., Ragab, A., Fournié, B., Sarda, L., and Chap, H. (1995) *Cell* **80,** 919–927
49. Kudo, I., Murakami, M., Hara, S., and Inoue, K. (1993) *Biochim. Biophys. Acta* **1170,** 217–231
50. Beers, S. A., Buckland, A. G., Koduri, R. S., Cho, W., Gelb, M. H., and Wilton, D. C. (2002) *J. Biol. Chem.* **277,** 1788–1793
51. Huhtinen, H. T., Grönroos, J. O., Grönroos, J. M., Uksila, J., Gelb, M. H., Nevalainen, T. J., and Laine, V. J. (2006) *APMIS* **114,** 127–130
52. Koduri, R. S., Grönroos, J. O., Laine, V. J., Le Calvez, C., Lambeau, G., Nevalainen, T. J., and Gelb, M. H. (2002) *J. Biol. Chem.* **277,** 5849–5857
53. Koprivnjak, T., Peschel, A., Gelb, M. H., Liang, N. S., and Weiss, J. P. (2002) *J. Biol. Chem.* **277,** 47636–47644
54. Gimenez, A. P., Wu, Y. Z., Paya, M., Delclaux, C., Touqui, L., and Goossens, P. L. (2004) *J. Immunol.* **173,** 521–530
55. Degousee, N., Ghomashchi, F., Stefanski, E., Singer, A., Smart, B. P., Borregaard, N., Reithmeier, R., Lindsay, T. F., Lichtenberger, C., Reinisch, W., Lambeau, G., Arm, J., Tischfield, J., Gelb, M. H., and Rubin, B. B. (2002) *J. Biol. Chem.* **277,** 5061–5073
56. Piris-Gimenez, A., Paya, M., Lambeau, G., Chignard, M., Mock, M., Touqui, L., and Goossens, P. L. (2005) *J. Immunol.* **175,** 6786–6791